Structural Engineering and Mechanics, *Vol. 60, No. 3 (2016) 507-527*
DOI: http://dx.doi.org/10.12989/sem.2016.60.3.507

Cyclic behavior of extended end-plate connections with shape memory alloy bolts

Nader Fanaie[a] and Morteza N. Monfared[*]

Department of Civil Engineering, K. N. Toosi University of Technology, Tehran, Iran

(Received November 18, 2015, Revised August 30, 2016, Accepted September 9, 2016)

Abstract. The use of shape memory alloys (SMAs) has been seriously considered in seismic engineering due to their capabilities, such as the ability to tolerate cyclic deformations and dissipate energy. Five 3-D extended end-plate connection models have been created, including one conventional connection and four connections with Nitinol bolts of four different prestress forces. Their cyclic behaviors have been investigated using the finite element method software ANSYS. Subsequently, the moment-rotation responses of the connections have been derived by subjecting them to cyclic loading based on SAC protocol. The results obtained in this research indicate that the conventional connections show residual deformations despite their high ductility and very good energy dissipation; therefore, they cannot be repaired after loading. However, while having good energy dissipation and high ductility, the connections equipped with Nitinol bolts have good recentering capability. Moreover, a connection with the mentioned specifications has been modeled, except that only the external bolts replaced with SMA bolts and assessed for seismic loading. The suggested connection shows high ductility, medium energy dissipation and very good recentering. The main objective of this research is to concentrate the deformations caused by cyclic loading on the connection in order to form super-elastic hinge in the connection by the deformations of the shape memory alloy bolts.

Keywords: end-plate connection; shape memory alloy; super-elastic behavior; cyclic performance; recentering

1. Introduction

The historical background of studying and assessing the behavior and design of connections in moment resisting frames against earthquakes goes back a few decades ago. Investigations on such connections started after the Northridge (California) and Kobe (Japan) earthquakes, when many steel buildings collapsed due to the fracture of welded regions in their beam-column welding connections. Since then, many studies have been conducted on the behavior and proper design of connections. The most important study was done by FEMA through a project known as SAC. This project involved many investigations and laboratory models, including two main phases of determining the reasons for welding connection rupture and finding the proper substitutive connection for use in earthquake resistant flexural frames. Accordingly, end-plate connections

∗Corresponding author, M.Sc., E-mail: m_nazari_civil@yahoo.com
[a]Ph.D., E-mail: fanaie@kntu.ac.ir

http://www.techno-press.org/?journal=sem&subpage=8 ISSN: 1225-4568 (Print), 1598-6217 (Online)

were accepted as the appropriate substitution in the second phase of the project. These new connections have shown proper seismic performance, having sufficient strength, ductility and rigidity (Adey, Grondin *et al*. 1997). The design strategy of connections with end-plates according to the principle of "strong connection-weak beam" usually results in the formation of inelastic deformations either in the beam (full strength connections) or in the connection (partial strength connections) after an earthquake. Both of these statuses are confronted with high economic costs and considerable difficulties during repair and reconstruction. Investigations have been conducted to overcome the defects resulting from residual deformations. The main aim was to incorporate post-tensioned high-strength bars into the connections in order to provide a self-centring mechanism (Ricles, Sause *et al*. 2002, Christopoulos, Filiatrault *et al*. 2002). In this regard, using shape memory alloys in the connections has drawn significant attention. Based on these studies, it can be said that the application of shape memory alloy of nickel-titanium (Nitinol) is the appropriate solution for confronting the relevant difficulties in seismic regions. The capability of shape memory alloys to tolerate cyclic deformations and their moderate energy dissipation during cyclic loading have made them appropriate components against earthquake loads (Lagoudas 2008, Abolmaali, Treadway *et al*. 2006). Several researches have been conducted on the use of shape memory alloys. Abolmaali, Treadway *et al*. (2006) studied the hysteresis behavior of T-stub connections with SMA bolts and observed proper energy dissipation and high recentering. Hu, Choi *et al*. (2011) suggested a new kind of connection for connecting beams to CFT columns, which applies SMA tendons inside the column section. DesRoches, Taftali *et al*. (2010) and Ellingwood, Taftali *et al*. (2010) modeled steel flexural frames equipped with shape memory alloy connections using finite element method and nonlinear time history analysis. They assessed the effects of such connections on the residual drift of stories and obtained appropriate results, such as considerable reduction of residual deformations. Ocel, DesRoches *et al*. (2004) applied martensitic SMA tendons and heated them. They obtained two results: 1) stability in the hysteresis responses; and 2) recovery of the residual deformations of the tip of the beam after heating (more than 50%) until the deformation of SMA tendons. A connection similar to Ocel's was experimented by Penar (2004). The obtained results indicated the good recentering capability of this kind of connection. Ma, Wilkinson *et al*. (2007) suggested another similar connection equipped with the mentioned alloys. They proposed connections with extended end-plate and SMA bolts. In this regard, in the modeling by finite element method, the austenite SMA bolts were replaced by ordinary high strength steel ones. Expectedly, high recentering and proper energy dissipation were reported by this study. Rofooei and Farhidzadeh (2011) conducted dynamic analysis on four flexural frames of different numbers of stories equipped with rigid connections, steel and super-elastic SMA bolts using finite OpenSees software. According to their results, impressive reduction was observed in the relative displacements of the stories as well as in the base sections of the frames equipped with SMA connections compared to those with conventional rigid connections.

Recently, Fang, Yam *et al*. (2014) did a follow-up of the studies of Ma *et al*. on connections with extended end-plate equipped with SMA bolts. In their research, they investigated eight laboratory samples, including one connection with high strength steel bolts and seven connections with Nitinol bolts. The objective of the research was to study the main specifications of moment connections such as stiffness, strength, ductility and equivalent viscous damping. The main parameters studied in the mentioned investigation were the length and diameter of SMA bolts. Moreover, the dimensions of the beam, column and end-plate were considered in such a way that all components of the connection excluding the bolts remained elastic during cyclic loading. In fact, super-elastic hinge was formed in the connection by SMA bolts.

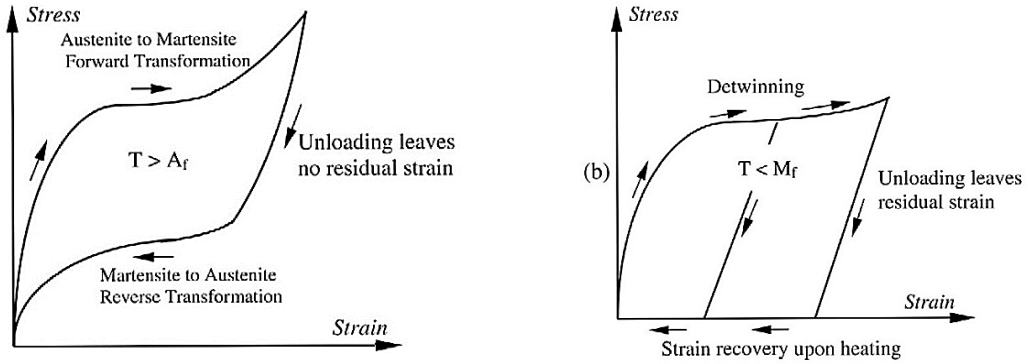

(a) SE for austenite (b) SME for martensite.

Fig. 1 The Stress-Strain responses for SMAs

Wang, Chan *et al*. (2015) proposed a novel connection by integrating superelastic SMA tendons with steel tendons between a H-shaped beam to a CHS column. Six full-scale prototype specimens with different combination of SMA and steel tendons were tested to evaluate the recentering capability and the energy dissipative performance. Test results showed that connections equipped with SMA tendons exhibit moderate energy dissipation, double-flag-shaped hysteresis loops and excellent recentering capability after being subjected to cyclic loads up to 6% interstory drift angle. They also examine the structural performance of joints between CHS column and I-beam equipped with SMA tendons and steel angles. For this purpose, two full-scale laboratory tests were conducted to investigate (1) the re-centering capability contributed by the SMA tendons and (2) the energy dissipative performance contributed primarily by the steel angles. Parallel numerical and parametric analyses through ANSYS were also conducted. Both experimental and numerical results confirmed the significance of the thickness of the steel angle and the initial prestress on the SMA tendons towards the connection's stiffness, re-centering and energy dissipative performance. A thinner angle resulted in lower connection stiffness and a lower energy dissipative ability, however a promising re-centering capability was guaranteed. Higher initial prestress on the SMA tendons also facilitates the re-centering performance (Wang, Chan *et al*. 2015).

2. The characteristics of shape memory alloys

Shape memory alloys have two unique specifications, the effect of shape memory and super-elasticity. These two behaviors can be formed by the conversions of the crystalline phase entitled martensite and austenite (Tyber, McCormick *et al*. 2007, McCormick, Tyber *et al*. 2007). Among different kinds of existing memory alloys, Nitinol (obtained from two elements, nickel and titanium) has drawn more attention in the research arena of civil engineering. When Nitinol experiences deformation at a temperature lower than the austenite phase (A_f), residual deformations will be observed after unloading. These deformations are mostly removed by heating the alloy up to a temperature higher than that of the austenite phase (A_f). This phenomenon is called shape memory effect, Fig. 1(b). On the other hand, if Nitinol alloy experiences deformation at a temperature higher than that of A_f, the created deformations are removed spontaneously after

unloading. Changing the crystallographic nature of the martensite phase during these inelastic deformations will cause energy dissipation. This phenomenon is known as super-elastic effect (1-a). Based on civil engineering perspective and more particularly seismic performances, the super-elastic behavior of these alloys have been considered mainly due to their valuable capabilities such as hysteresis damping and spontaneous recentering of deformations. Comprehensive up-to-date studies on the application of these alloys in civil engineering have been done (Saadat, Salichs *et al*. 2002, DesRoches and Smith 2004, Wilson and Wesolowsky 2005, Song, Ma *et al*. 2006).

3. Research procedure

This research is a follow-up of the investigations conducted on the use of SMA bolts in steel moment connections with end-plates. Based on available information, first, a 3-story building and its ordinary elements, including beams and columns, were modeled according to the conditions of the loading code ASCE (2006). Then, high strength steel bolts, needed for the connection, were designed using AISC design guide (2004). The same connection was designed again with SMA bolts, with the consideration that the bending capacity of the beam is higher than the capacity of all bolts. In this regard, the beam and column of the connection remained elastic up to the end, and a super-elastic hinge was created in the connection by the deformation of SMA bolts instead of plastic hinge formation in the beam. The end-plate was designed in a thick form in order to prevent the formation of prying action. Then, the behavior of this connection was assessed for different values of pre-stressing: 40, 50, 60 and 70% of tension yield of SMA bolts. These connections were evaluated for their seismic specifications such as ductility, energy dissipation, stiffness, strength and recentering. Next, the optimum SMA connection was selected considering its pre-stressing value. Eventually, a new connection was assessed in which only the bolts of the external rows are of SMA.

The objective of suggesting such a hybrid connection is to introduce a connection with appropriate behavior. From one hand, strain demand exists in the external bolts more than that of internal ones in this kind of connection. On the other hand, the bolts of these alloys show super-elastic behavior in the presence of relatively high strain. Expectedly, using SMA bolts only in the external rows is economically a logical and optimum assumption. In the following sections, the effects of the pre-stressing force of SMA bolts are investigated on the behavior and response of moment-rotation, energy dissipation and ductility of this kind of connection.

4. Numerical simulation

The modeled connections and the procedure of modeling are introduced in order to investigate the behavior of each connection. Accordingly, a 3-dimensional model was prepared by finite element method using ANSYS software. This program contains super-elasticity and shape memory effects by itself (Auricchio 2001). In this section, three different general finite element models of connections are presented, including conventional connection with steel bolts, connection with SMA bolts and connection with hybrid or dual bolts. The designed connection is the kind with stiffened 8-bolt end-plate (8ES). In order to simplify the reference to the types of connections, all connections were entitled HS, Full SMA and Hybrid. On the other hand, four different values of pre-stressing were created in the bolts of the Full SMA connection to obtain the

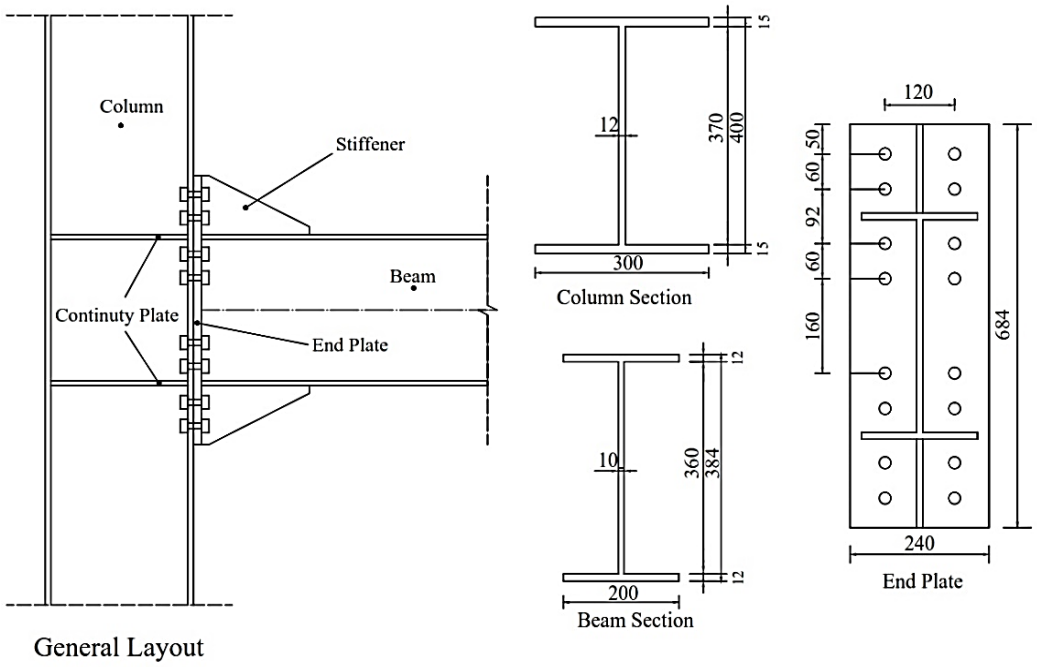

Fig. 2 The details and geometrical dimensions of connection elements

results of each value. Therefore, another sub-entitling was considered. For example, Full SMA-50 connection corresponds to the connection with total SMA bolts of 0.5*fy* pre-stressing. It should be mentioned that in the hybrid connections, only the external rows of bolts are of SMA (8 bolts of 16 bolts), while the internal ones are of high strength steel bolt. The details and dimensions of connection elements are presented in Fig. 2. The dimensions of the beam, column, end-plate and stiffeners are the same in all connections. The models are different just in the sizes and material of the bolts. Building steel of ST37 was used for all elements excluding the bolts which are of high strength steel 8.8 grade (ASTM 325). The specifications of SMA bolt materials have been presented in Tables 1-2. The diameter of steel bolts for HS connection is 21 mm; it is calculated according to AISC design code. This value is 15mm for Full SMA connection in which the design moment has been reduced logically. It should be mentioned that steel bolts of the same axial stiffness were used in the hybrid connection for substituting high strength steel bolts with SMA bolts. This process is presented in Eq. (1). Therefore, the diameter was considered as 7 mm with a little connivance. These three connections are geometrically different from each other only in the diameters of their bolts.

$$K_{(SMA,bolt)} = K_{(Steel,bolt)} \Rightarrow \left(\frac{EA}{L}\right)_{(SMA)} = \left(\frac{EA}{L}\right)_{(Steel)}$$
$$d_{(Steel)} = d_{(SMA)}\sqrt{\frac{E_{(SMA)}}{E_{(Steel)}}} = 15\sqrt{\frac{42}{200}} = 6.88mm \quad (1)$$

Table 1 Material properties of connection elements.

Material	Modulus of elasticity (GPa)	Poisson's ratio	Yielding stress (MPa)	Ultimate stress (MPa)
ST37	200	0.3	240	370
HS 8.8 (ASTM 325)	200	0.3	640	800
SMA	42	0.33	370	500

Table 2 Material specifications of SMA bolts

Starting stress of forward phase transformation (σ_{MS})	360 MPa
Final stress of forward phase transformation (σ_{Mf})	450 MPa
Starting stress of reverse phase transformation(σ_{AS})	280 MPa
Final stress of reverse phase transformation (σ_{Af})	130 MPa
Maximum residual strain (ε_L)	0/05
Parameter measuring the difference between material response in tension and compression (α)	0

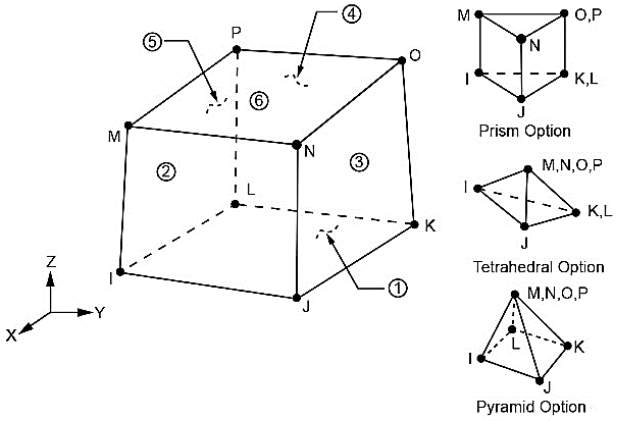

Fig. 3 Configuration of the solid 185 element

The material nonlinearities of steel member were represented by the kinematic hardening and bilinear elasto'-plastic model and the von Mises yield criterion with 5% tangent modulus/elastic modulus ratio. A cubic element (solid 185) has been used for all steel elements. The cubic element can model both super-elastic and shape memory behavior; thus, it is used for SMA bolts as well. This element has 8 nodes, each of which has three degrees of freedom in *X*, *Y* and *Z* directions, Fig. 3. Moreover, it can be converted to four different shapes for meshing by merging different nodes. Super-elastic behavior was modeled in ANSYS software according to the model presented by Auricchio (2001). In their model, the material has the capability of tolerating large deformations without showing residual deformation in the isothermal situation.

The lengths of the cantilever beam and column are 1500 mm and 3200 mm respectively. The column was considered fixed at the top and bottom. In reality, the connected components are related to each other frictionally. In the software as well, they are connected to each other frictionally with a friction coefficient of 0.2. Moreover, they are totally constrained by bond

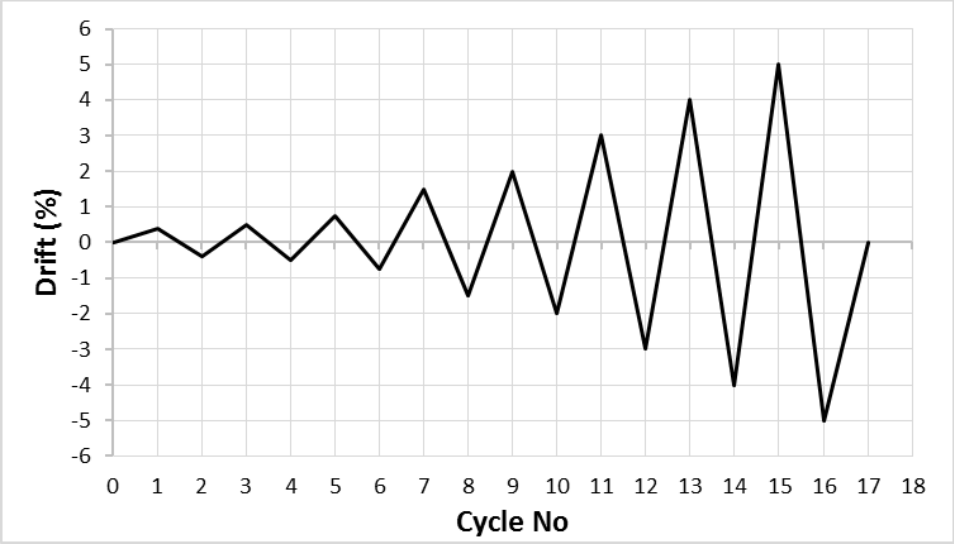

Fig. 4 Beam tip drift vs. cycle number for modified loading

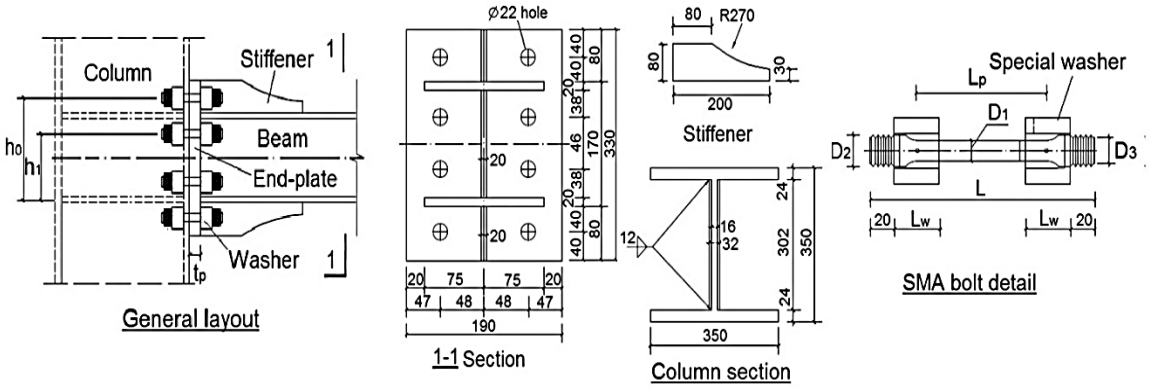

Fig. 5 Configuration of SMA-D10-240-d connection for using in the verification

contact order instead of modeling the welds of sections. The models were loaded using SAC loading protocol, which is a displacement control loading, Fig. 4. In the finite element software, loading was applied statically to the end of the cantilever beam up to the loading step of 5%. It should be mentioned that a major difference between the loadings of connections relative to the loading protocol was considered; i.e., only the first loading cycle was applied to reduce the calculation attempts.

4.1 Verification of FE models

A sample of the laboratory results of Fang, Yam *et al*. (2014) was selected to verify the modeling. Its details are presented in Fig. 5. The numerical and laboratory results are accordant with acceptable accuracy, as shown in Fig. 6.

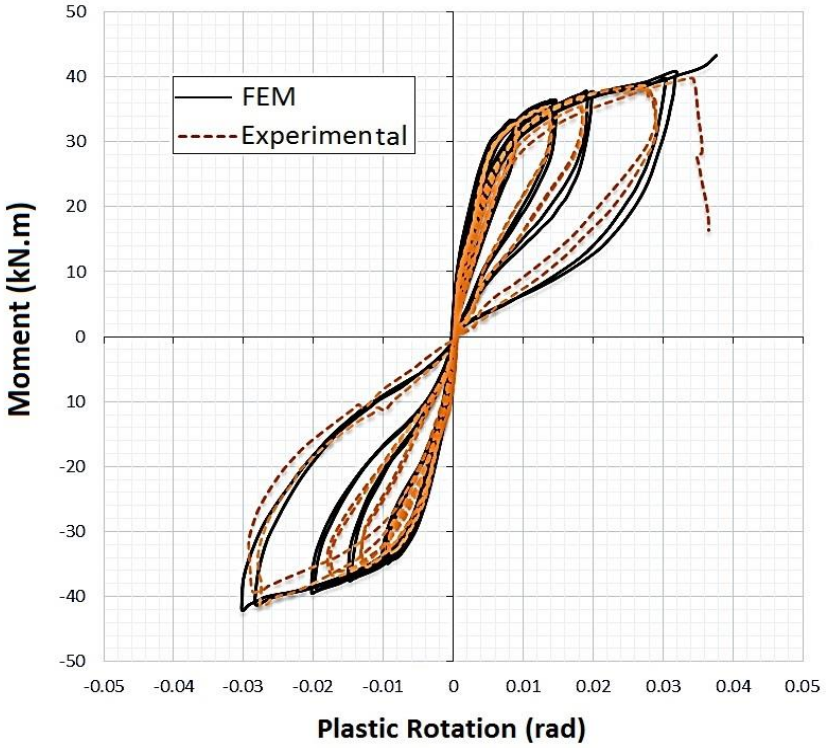

Fig. 6 Comparing the numerical and experimental results

4. Mechanical behavior of the connections

4.1 General

The main cyclic specifications, including moment-rotation response, ductility, stiffness, strength, energy dissipation and recentering, have been extracted for each connection.

4.2 Moment-rotation response

For a typical cantilever system as used in this study, the plastic rotation can be obtained by deducting the elastic deformation of the beam from the total deformation, as presented in Eq. (2)

$$\theta_p = \frac{\Delta - F / k_e}{L} \tag{2}$$

where θ_p=plastic rotation, Δ=displacement (e.g., beam tip displacement), F=applied load, K_e=elastic stiffness of the beam and L=arm length.

The plastic moment-rotation response of HS connection shown in Fig. 7 expectedly has stable and wide hysteresis loops, indicating good ductility and excellent energy dissipation, as subsequently explained. A slight plastic deformation is seen in the first loading cycle. It increases with increasing displacement values of the beam end. HS connection presents stable hysteresis

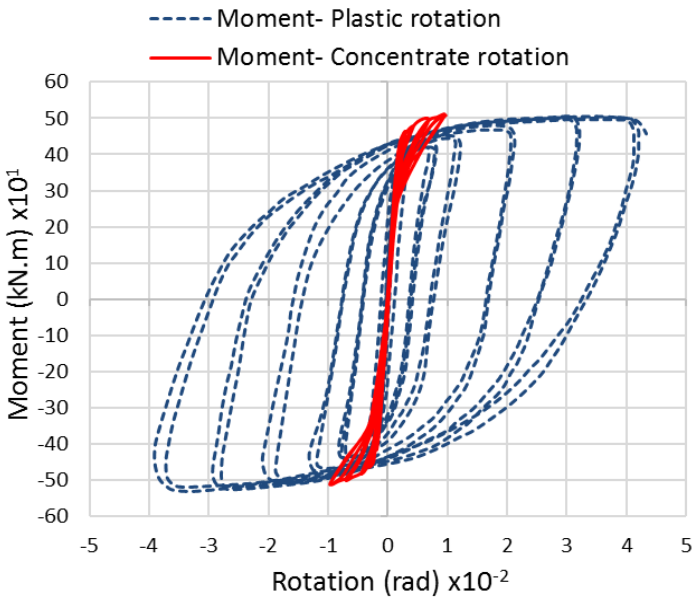

Fig. 7 Moment-rotation response of HS connection

response up to 5% loading step. The maximum moment tolerated by this connection is 506.1 kN.m. According to Fig. 7, stiffness degradation of the connection is observed in cycles with higher drifts (after 2% loading step) due to the yielding of the beam stiffener edge in the plastic hinge region. Moreover, the maximum plastic rotation formed in the connection is 0.042 radian.

Fig. 7 presents the moment-concentrated rotation response of HS connection in the form of a solid line. In order to calculate this rotation, the relative displacement of the top and bottom of the end-plate are divided by their distances (the height of the end plate), indicating that the rotation of the connection is caused by changing the lengths of the steel bolts. According to this figure, the concentrated rotation with maximum value of 0.01 radian is relatively small comparing to the whole rotation or plastic rotation of HS connection. The reason for the difference between the responses of moment-plastic rotation and moment-concentrated rotation is that the steel bolts are still in their elastic regions; i.e., they have not entered the plastic region. This fact expresses the ordinary philosophy that exists in the design of such connections in the AISC code.

Fig. 8 also presents the moment-plastic rotation and moment-concentrated rotation responses of SMA connections. Unlike HS connection, a very slight difference is seen between the responses of moment-plastic rotation and moment-concentrated rotation. This phenomenon can be justified because the rotation of the connection is mainly supported by SMA bolts by increasing their lengths. As these deformations are returned by unloading, plastic deformation is slightly formed. All SMA connections remain in their elastic regions up to a loading step of 0.75% without forming considerable hysteresis loops. However, for higher loading steps, the moment-rotation response gradually approaches its flag form due to the entrance of SMA bolts into the martensite phase. A noteworthy point from these responses is that the flag shape of hysteresis loops are formed earlier in the models with higher pre-stressing values.

For example, in the model of Full SMA-40 connection, the elastic part of the flag response is clearer comparing to that of others. As the pre-stressing values increase, the flag shape loops of the

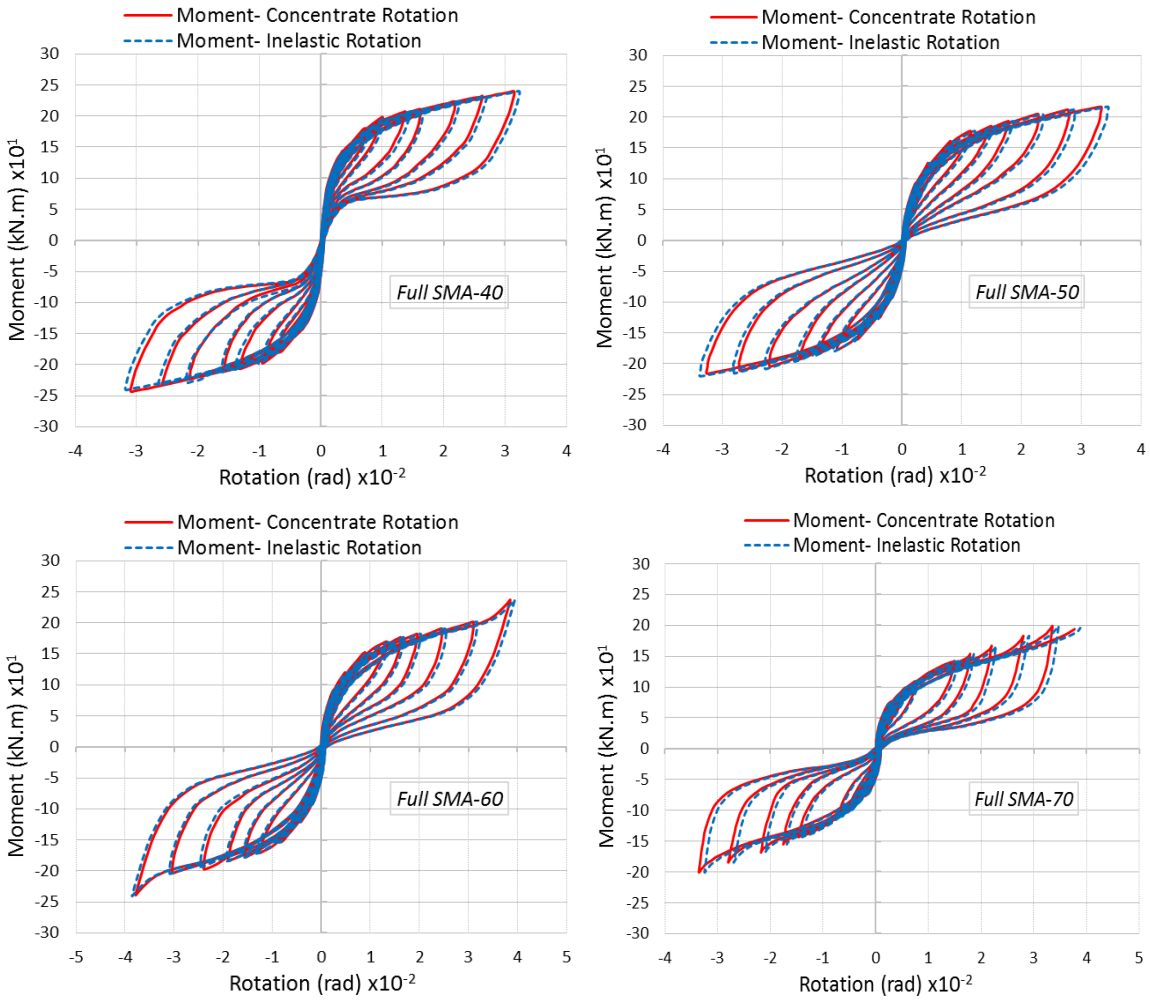

Fig. 8 Moment-rotation response of Full SMA connections models

moment-rotation response become closer to the horizontal axis and the elastic part is gradually removed. This phenomenon is justified because by increasing the pre-stressing force, the behavior of the bolts is not initiated from the beginning point of their stress-strain responses and a mutation has occurred there. It means that by increasing the pre-stressing force, the martensite phase starts earlier in the SMA bolts. Regarding Full SMA-40 (Fig. 8), the elastic behavior is considerable at the beginning of the stress-strain response, besides observing super-elastic behavior. In the Full SMA-40, Full SMA-50 and Full SMA-60 connections, maximum moments are 239.4 kN.m, 216 kN.m and 236 kN.m respectively, while the maximum values of concentrated rotation are 0.0314 radian, 0.0345 radian and 0.0393 radian respectively.

The value of the maximum moment is higher in the Full SMA-60 comparing to that of Full SMA-50. According to the figure, the reason is that in the last cycles of loading, particularly the last two cycles, SMA bolts enter their post-elastic regions (spiky part), which naturally results in increase of strength of the connection. However, the rotation of the connection still increases with

increasing pretension force of the bolt. Eventually, an abrupt increase in the strength of the connection is observed in the final cycles of Full SMA-70 due to the post-elastic behavior of Nitinol bolts, such that its maximum moment is 200 kN.m and maximum rotation is 0.0385 radian. The main difference between this connection and Full SMA-60 is that by increasing the stress values created in the bolts (including the resultant of pre-stressing force and the force transmitted from beam), the stress in the last row exceeds its allowable value (500 MPa), despite the existence of post-elastic hardening, and causes rupturing of the bolt and finally, failure of the connection.

Different specifications of the cyclic behavior of SMA connections have been studied and compared based on the different percentages of pre-stressing. Now, the focus is on the suggested hybrid connection. For this purpose, a connection with optimum percentage of pre-stressing is selected. Full SMA-60 has the highest ductility, strength and energy dissipation comparing to others, as presented in the following sections. Therefore, it can be chosen as the connection with optimum percentage of pre-stressing. Despite not being the best regarding some capabilities, such as recentering and hardening, it is still selected due to the slight difference in its recentering and hardening capabilities comparing to the average recentering ability of other SMA connections.

According to Fig. 9, the response of moment-rotation for Hybrid connection has also flag shape like all other SMA connections. The most important difference between the responses of moment-rotation of this connection and Full SMA connections is its relatively high residual deformation after unloading in each step. In this connection, maximum tolerated moment and rotation are 284.53 kN.m and 0.04 radian respectively. In the first loading step, small hysteresis loops are formed, like other previous connections. These hysteresis loops, which tend more towards flag shape, become larger and more recognizable with increasing loading. The maximum values of moment and rotation are presented in Table 3 for all 6 connections.

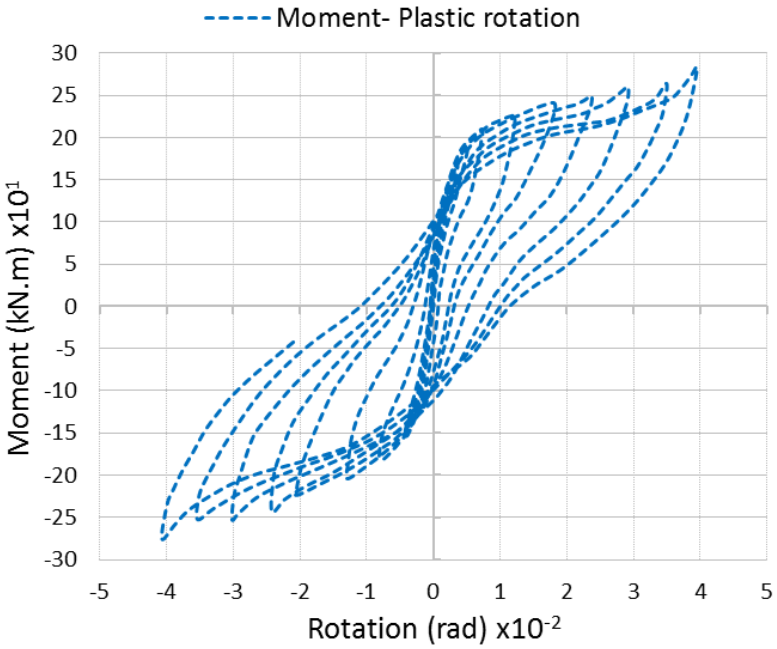

Fig. 9 Moment-plastic rotation response of hybrid connection

Table 3 Maximum values of moment and rotation for connections

Connection model	Maximum moment (kN.m)	Maximum rotation (rad)
HS	506.1	0.042
Full SMA-40	239.4	0.0314
Full SMA-50	216	0.0345
Full SMA-60	236	0.0397
Full SMA-70	200	0.0385
Hybrid	284.53	0.04

Figs. 10-11 present the distribution of equivalent von Mises stress and equivalent plastic strain for all 5 connections. According to these figures, in the SMA connections, unlike HS connection, the beam and column remain in their elastic regions. Moreover, in the SMA connections, the deformations are mostly controlled by SMA bolts through super-elastic behavior. Based on Figs. 10-11, in the HS connection, the plastic hinge is formed in the final region of the connected beam near the stiffeners of the end-plate. Meanwhile, the bolts still remain in their elastic regions and do

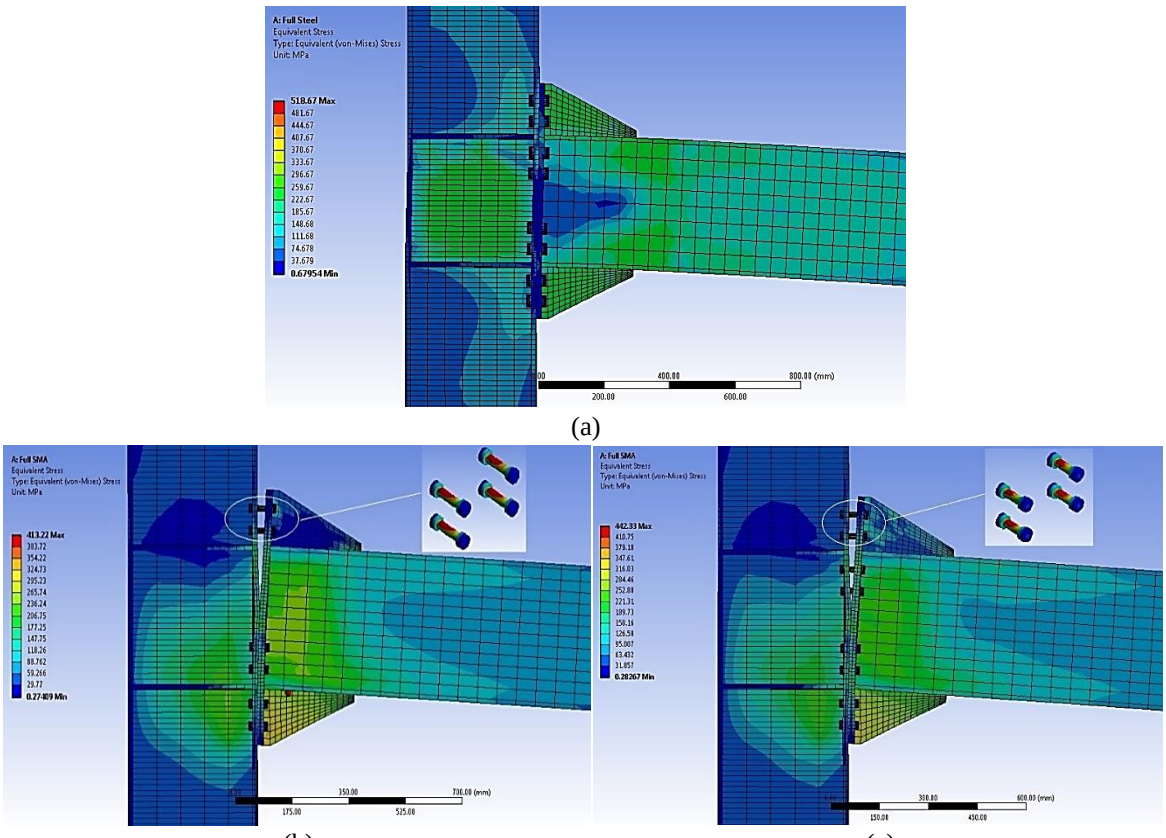

Fig. 10 Distribution of equivalent von Mises stress for the connections: (a) HS, (b) Full SMA-40, (c) Full SMA-50, (d) Full SMA-60, (e) Full SMA-70

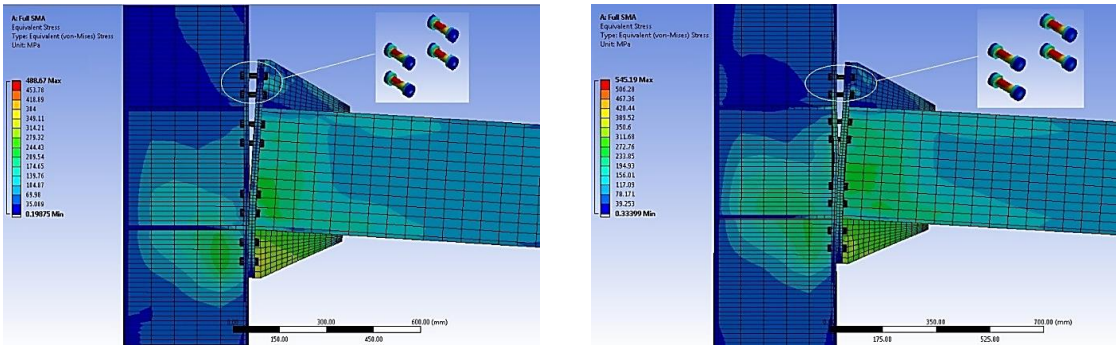

(d) (e)

Fig. 10 Continued

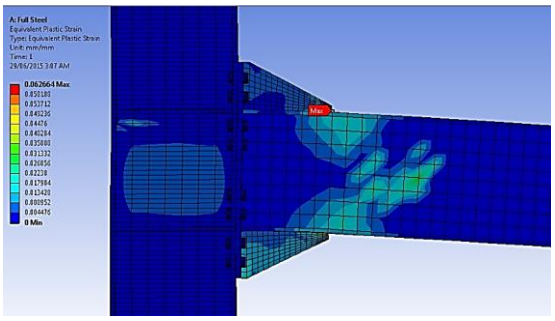

(a)

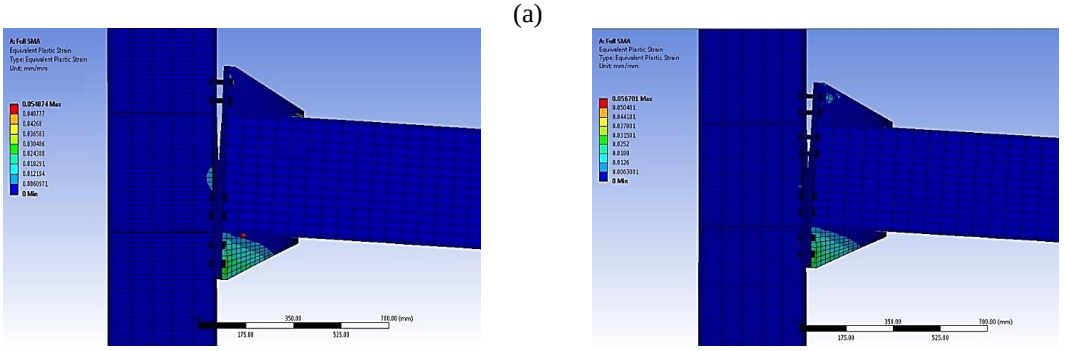

(b) (c)

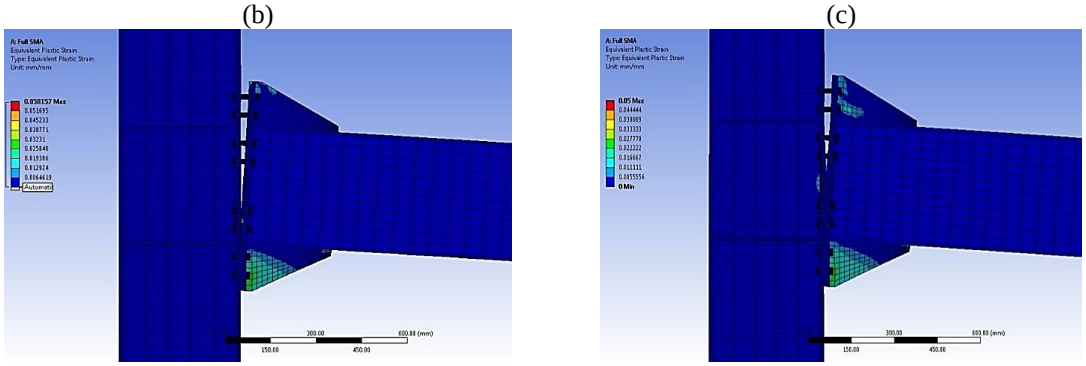

(d) (e)

Fig. 11 Distribution of equivalent plastic strain for the connections: (a) HS, (b) Full SMA-40, (c) Full SMA-50, (d) Full SMA-60, (e) Full SMA-70

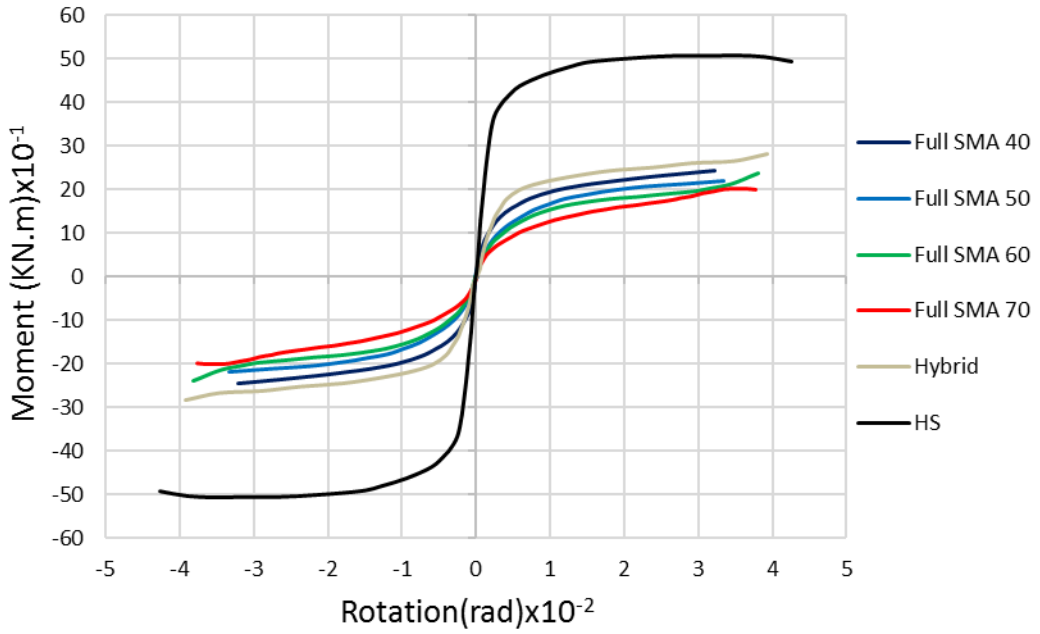

Fig. 12 Back bone curve for modeled connections

not experience plastic deformation and yielding. In SMA connections, local yield is observed in the stiffeners of the end-plate, which becomes more observable with increasing the moment caused by the bolts.

4.3 Back bone curve

Back bone curve is an important and applicable curve derived from hysteresis moment-rotation response and known as cyclic envelope curve. Fig. 12 presents the envelope of moment-rotation responses plotted for the 5 mentioned connections. According to the figure, the initial stiffness of the HS connection is higher comparing to SMA connections. The reasons are as follows: 1) the design philosophy of these connections; and 2) the high stiffness of steel bolts in such connections due to their high elasticity modulus.

4.4 Ductility

Connections are generally expected to have sufficient ductility for tolerating seismic loads. According to Eurocode 8 (2005), connections under seismic loading should be designed in such a way that the rotational capacity of the plastic hinge region will not be lower than 0.035 and 0.025 radian for high and medium classes of ductility respectively. Based on the seismic provision of AISC (2005), the connections should be designed in such a way that the special and intermediate moment frames, equipped with them, can tolerate minimum inter story drift angles of 0.04 and 0.02 radian respectively. Two different terms have been presented for ductility demand in Eurocode 8 and AISC, namely rotational capacity of plastic hinge region and inter story drift angle respectively. The relative displacement word “drift” is used from now in this study. According to

Table 4 Classifying the modeled connections based on ductility

Connection model	Ductility group based on **AISC**	Ductility group based on **Eurocode 8**
HS	high ductility	high ductility
Full SMA-40	medium ductility	medium ductility
Full SMA-50	medium ductility	medium ductility
Full SMA-60	high ductility	high ductility
Full SMA-70	medium ductility	high ductility
Hybrid	high ductility	high ductility

Eurocode 8, Hs, Full SMA-60 and Full SMA-70 are connections of high ductility, while Full SMA-50 and Full SMA-40 are of medium ductility. Classifying these connections based on AISC code, HS and Full SMA-60 (with slight connivance) are of high ductility, while the others are of medium ductility values. Therefore, HS connection has the highest ductility values due to its design philosophy. In other words, the main reason for higher ductility in the conventional connections is the yielding of the beam in the plastic hinge. The connections are classified according to AISC and Eurocode 8 and briefly presented in Table 4.

4.5 Strength and stiffness

Connections can generally be classified based on their strength and stiffness; i.e., a connection can be categorized as pinned, semi-rigid and rigid with respect to its initial rotational stiffness and its *EI/L*; where, *E*, *I* and *L* are modulus of elasticity, second moment of area and beam span respectively. According to Eurocode 3 (2005), a connection is simple or pinned when its initial rotational stiffness is lower than 0.5EI/L. However, if its initial rotational stiffness is higher than 25EI/L, then it is considered as rigid. A connection with initial stiffness between these two values is semi-rigid. Concerning its strength, a connection can be classified as pinned, partial strength and full strength based on the designed plastic flexural strength of all connected elements. A connection is nominally pinned if its strength (i.e., moment capacity) does not lead to significant moments which might adversely affect the members or the whole structure, while it is a full-strength connection if its strength is larger than the design plastic moment resistance of the connected member. A connection is full strength if its strength is higher than the whole plastic moment of the elements. A connection with intermediate strength is partial strength. These classifications are different from that of AISC and other codes, though with the same principle basis.

In this research, relatively early nonlinear behavior was observed in SMA connections. Therefore, secant stiffness in the moment-rotation response concentrated in the initial cycle (0.375%) can be an appropriate and logical estimation of their initial rotation stiffness (K_{sec}). This is obtained by dividing the maximum value of tolerated moment by the maximum value of concentrated rotation of the connection in the first loading cycle. Tables 5-6 present 6 kinds of connections, classified with respect to the stiffness and strength. EI/L can be calculated for the connected beam as follows:

$$E = 2\times10^{8} kN/m^{2}, I = 1.972\times10^{-4} m^{4}, L = 2\times1.5 = 3m \Rightarrow \frac{EI}{L} = \frac{2\times10^{8}\times1.972\times10^{-4}}{3} = 13147\, kN.m \quad (3)$$

Table 5 Classifying connections with respect to their rotational stiffnesses based on Eurocode 3.

Connection	K_{Sec}	$K_{sec}/(EI/L)_{beam}$	classification
HS	421625	32/07	Rigid
Full SMA-40	192250	14/62	Semi Rigid
Full SMA-50	178272	13/56	Semi Rigid
Full SMA-60	154320	11/74	Semi Rigid
Full SMA-70	131732	10/02	Semi Rigid
Hybrid	215740	16/04	Semi Rigid

Table 6 Classifying the modeled connections with respect to their strengths based on Eurocode 3

Connection model	Mmax	Mmax/Mp,beam	Classification
HS	506.18	1.83	Full Strength
Full SMA-40	239.42	0.87	Partial Strength
Full SMA-50	216.12	0.78	Partial Strength
Full SMA-60	236.65	0.86	Partial Strength
Full SMA-70	201.10	0.73	Partial Strength
Hybrid	284.53	1.029	Full Strength

The values of $M_{p,\,beam}$, presented in Table 6, indicate the plastic moment of connected beam and are calculated as follow

$$M_{p,beam} = (F_y)(Z_{xb}) = (2400)(1152) = 2764800\,kg.cm = 276.48kN.m \tag{4}$$

Based on Table 5, the hybrid connection has a higher stiffness comparing to the Full SMA-60 connection in which 60% of stress yielding of SMA bolts are pre-stressed. The increase in the stiffness of the hybrid connection is due to the existence of steel bolts. The increase is as much as 37%, but still the connection acts as semi-rigid. However, the hybrid connection has greater mutation concerning its strength, moving from the group with partial strength to the full strength group. The reason for increasing the strength is the presence of high strength steel bolts. Therefore, the steel bolts with the assumption of the same axial stiffness was substituted for internal Nitinol bolts, while their yielding stress values were higher than those of Nitinol bolts.

4.6 Energy dissipation

For a better understanding of the performance of connections, their energy dissipations are assessed using their equivalent viscous damping values and expressed in this section. Equivalent viscous damping is defined in Eq. (5) (Speicher, DesRoches *et al*. 2011) as follow

$$\xi_{eq} = \frac{E_D}{4\pi E_{so}} = \frac{E_D}{2\pi K_s \delta_{\max}^2} \tag{5}$$

Where ED is the energy dissipated in a complete loading cycle (the area of moment-rotation response of a cycle); E_{so} is the energy absorbed by a linear system which simultaneously has maximum deformation (here rotation) and corresponding force. The value of equivalent viscous damping has been calculated for the first cycle of each loading step and presented in Fig. 13.

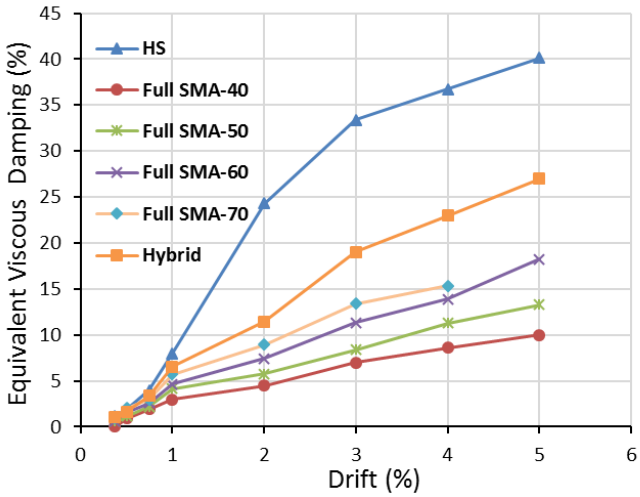

Fig. 13 Equivalent viscous damping as per each loading step for the first cycles

According to this figure, the damping of connections generally increases with increasing rotation of the beam end. The HS connection has the highest percentage (41%) of equivalent viscous damping due to the yielding of the beam, which results in the formation of stable and wide hysteresis loops. Regarding SMA connections, the more the pre-stressing force, the more the value of equivalent viscous damping. This phenomenon can be explained as the more the pre-stressing force increases, the wider the hysteresis loops obtained from more development of phase transformation loops of SMA bolts.

For Full SMA-70 connection model, the damping of the system is higher than those of other SMA connections up to the loading step of 4%. However, the last loop has not been accounted in the calculations due to the rupturing of bolts in the last step. According to Fig. 13, the hybrid connection has proper damping. Moreover, it has maximum equivalent viscous damping of 26.7% in its last cycle. This connection has higher energy dissipation in comparison with Full SMA connections and lower energy dissipation in comparison with that of HS ones. It can be said that the energy dissipation of this connection is between the energy dissipations of connections with steel bolts and those with SMA bolts.

4.7 Recentering

Recentering of connections can be determined by the values of residual rotations. Fig. 14 presents the accumulated rotation for the first cycle of each loading and unloading steps. According to this figure, the recentering capacity of HS connection is very low and the created deformations are nearly all plastic and permanent. The reason for this fact is the yielding of beam and partial yielding of other elements of the connection, excluding the bolts which remain in the elastic region. Unlike conventional connections, almost all deformations created in the SMA connections after each unloading step approach to zero, and the connections return to their initial statuses (self- centering phenomenon). It is obvious that the reason for this recentering mechanism is the super-elastic behavior of SMA bolts. According to Fig. 14, residual plastic rotation increases with increasing loading steps. The reason for this phenomenon is that with increasing loading steps

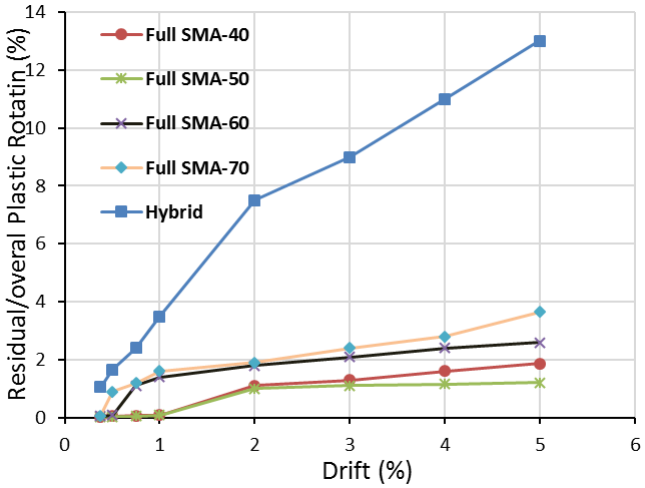

Fig. 14 Residual plastic rotation for each loading step of the connections

and applied external force, other elements such as the beam, column and stiffeners experience slight yielding, which causes the deformations or low residual rotations in the connection. In the SMA connections, with increasing pre-stressing force, the residual deformations also increase correspondingly. In fact, it can be said that with increasing the pre-stressing force, the strength of the moment of all bolts also increases for all SMA connections excluding Full SMA-50. This brings the stresses existing in other elements of the connection close to their yielding stresses and subsequently creating slight residual deformations in the connection. However, in Full SMA-50 connection, increasing the pre-stressing force does not result in an increase in the strength of the moment of the connection; it causes its reduction and therefore, lowers the residual deformations in this connection.

The residual rotations for hybrid connection are more considerable comparing to those of Full SMA connections, but the values are much lower than those of plastic residual rotation of HS connection. The main source of plastic rotation for this connection is the plastic deformations caused by steel bolts. Although other elements such as the connection beam enter the plastic region slightly, the plastic rotation of the hybrid connection is not considerable up to 1% loading step, after which it increases more severely.

5. Conclusions

• The conventional connections with high strength steel bolts, designed according to AISC code, possess high ductility, excellent energy dissipation and large residual deformations during cyclic loading, regarding their moment-rotation responses. This is because the philosophy which governs the designing of such connections was followed, based on the stronger design of connection relative to the connected beam. It means that the beam yields in the pre-determined plastic hinge before the bolts experience any yield or rupture. Therefore, the beam controls the behavior of the connection and prevents its failure from the bolts regions. However, the high residual deformations formed in the connection frustrate repair capability.

The beam cannot be used after several loadings. Connections with such behavior are categorized as those of full strength and rigidity.

• End-plate connections, in which SMA bolts are used, have the specifications of proper ductility and medium energy dissipation. However, their apparent features, strain recentering, prevent the formation of residual deformations (rotation) in the connection. This causes the improvement of performance and reduction of repairing costs after earthquake or loading.

• The connections equipped with SMA bolts are mostly placed in the group of partial and semi-rigid strength connections. These connections have lower stiffness comparing to those of other similar ones, due to the lower modulus of elasticity of SMA material in comparison with that of steel (1/3-1/5). Regarding the back bone responses derived for the connections, the initial stiffness of SMA connections is lower than that of HS.

• In Full SMA connections, ductility and dissipation energy (calculated by the criterion of equivalent viscous damping) generally increase with increasing pre-stressing force. The ascending trends of ductility and damping are continued up to 60% pre-stressing. In the connection with 70% pre-stressing, the bolts of the connections experience rupture in the 5% loading step.

• Regarding the bolts of SMA connections, the moment strength of the connection increases gradually when the pre-stressing force increases. This phenomenon happens because the post-elastic hardening of the bolts in the strains is higher than 0.05. By applying more pre-stressing force, the initiation of the stress-strain behavior of Nitinol bolts will not be in the beginning regions. Therefore, they reach the spiky parts of the stress-strain diagram, which finally result in an increase in the whole strength of the connection.

• Concerning the 4^{th} result, increasing the pre-stressing force of the bolts in the last loading step results in increasing resultant moment of all bolts (moment of connection), bringing it close to the plastic moment of beam. This causes slight yielding in other elements of the connection, such as beams and stiffeners. Therefore, the residual deformations also increase with increasing pre-stressing force. It means that as the pre-stressing increases, lower recentering is observed for the whole connection. It should be mentioned that the recentering capacity is very high, nearly 96.2%, even for Full SMA-70 connection.

• The bolts are modeled with different percentages of pre-stressing for the connections with SMA bolts. Accordingly, the connection with 60% pre-stressing shows the best performance. This optimum pre-stressing value has been selected considering higher ductility, better energy dissipation and appropriate recentering in the SMA bolts.

• After selecting the optimum pre-stressing value, which is 60% of the yielding stress of Nitinol bolts, a hybrid connection was modeled such that only the external bolts are SMAs. This connection presents stable hysteresis responses.

• Regarding its ductility, hybrid connection is placed in the group of connections with high ductility (with rotation of nearly 0.04 radian, almost equivalent to Full SMA-60). Moreover, the percentage of viscous damping of this connection is between those of Full SMA and HS.

• The suggested hybrid connection could be a proper substitution for conventional connections and even the connections with SMA bolts in high seismic regions. Moreover, concerning the high cost of using shape memory alloys, the suggested connection could be the optimum and logical selection due to its appropriate seismic specifications, such as high ductility, good energy dissipation and proper recentering.

References

Abolmaali, A., Treadway, J., Aswath, P., Lu, F.K. and McCarthy, E. (2006), "Hysteresis behavior of t-stub connections with superelastic shape memory fasteners", *J. Struct. Eng.*, **62**, 831'-8.

Adey, B.T., Grondin, G.Y. and Cheng, J.J.R. (1997), "Extended end plate moment connections under cyclic loading**"**, Ph.D. Dissertation, University of Alberta, Alberta, Canada.

AISC (2004), Extended end-plate moment connections, seismic and wind applications; Second Edition, AISC/ Steel Design Guide 4.

AISC (2005), Seismic provisions for structural steel buildings, Chicago, American Institute of Steel Construction.

ASCE (2006), Minimum design load for building and other structures, ASCE /SEI 7-05.

Auricchio, F. (2001), "A robust integration-algorithm for a finite strain shape memory alloy super-elastic model", *Int. J. Plast.*, 17971-90.

Christopoulos, C., Filiatrault, A., Uang, C.M. and Folz, B. (2002), "Posttensioned energy dissipating connections for moment-resisting steel frames", *J. Struct. Eng.*, **128**(9), 1111-20.

DesRoches, R. and Smith, B. (2004), "Shape memory alloys in seismic resistant design and retrofit: a critical assessment of the potential and limitations", *J. Earthq. Eng.*, **8**(3), 415-29.

DesRoches, R., Taftali, B. and Ellingwood, B.R. (2010), "Seismic performance of steel frames with shape memory alloy connections, part I-analysis and seismic demands", *J. Earthq. Eng.*, **14**(4), 471-86.

Ellingwood, B.R., Taftali, B. and DesRoches, R. (2010), "Seismic performance of steel frames with shape memory alloy connections, part II-probabilistic seismic demand assessment", *J. Earthq. Eng.*, **14**(5), 631-45.

Eurocode 3 (2005), Design of steel structures, EN 1993-1-8:2005ww: European committee for standardization, Brussels.

Eurocode 8 (2005), Design of structures for earthquake resistance—part 1: general rules, seismic actions and rules for buildings, EN 1998-1:2004 Eurocode 8: European Committee for Standardization.

Fang, C., Yam, M.C., Lam, A.C. and Xie, L. (2014), "Cyclic performance of extended end-plate connections equipped with shape memory alloy bolts", *J. Constr. Steel Res.*, **94**, 122-136.

Hu, J.W., Choi, E.S. and Leon, R.T. (2011), "Design, analysis and application of innovative hybrid PR connections between steel beams and CFT columns", *Smart Mater. Struct.*, **20**(2), 25019-33.

Lagoudas, D.C. (2008), *Shape memory alloys: modeling and engineering applications*, Springer, USA.

Ma, H.W., Cho, C. and Wilkinson, T. (2008), "A numerical study on bolted end-plate connection using shape memory alloys", *Smart Mater. Struct.*, **41**(8), 1419-26.

Ma, H.W., Wilkinson, T. and Cho, C. (2007), "Feasibility study on a self-centering beam-to-column connection by using the superelastic behavior of SMAs", *Smart Mater. Struct.*, **16**(5), 1555-63.

McCormick, J., Tyber, J., DesRoches, R., Gall, K. and Maier, H.J. (2007), "Structural engineering with NiTi. II: mechanical behavior and scaling", *J. Eng. Mech.*, **133**, 1019-29.

Ocel, J., DesRoches, R., Leon, R.T., Hess, W.G., Krumme, R., Hayes, J.R. and Sweeney, S. (2004), "Steel beam'-column connections using shape memory alloys", *J. Struct. Eng.*, **130**(5), 732-40.

Penar, B.W. (2005), "Recentering beam'-column connections using shape memory alloys", Master thesis school of civil and environmental engineering, Georgia Institute of Technology, Georgia.

Ricles, J.M., Sause, R., Peng, S.W. and Lu, L.W. (2002), "Experimental evaluation of earthquake resistant Post-tensioned steel connections", *J. Struct. Eng.*, **128**(7), 850-9.

Rofooei, F.R. and Farhidzadeh, A. (2011), "Investigation on the seismic behavior of steel MRF with shape memory alloy equipped connections", *The Twelfth East Asia-Pacific Conference on Structural Engineering and Construction*, **14**, 3325-3330.

Saadat, S., Salichs, J., Noori, M., Hou, Z., Davoodi, H., Bar-On, I. ... and Masuda, A. (2002), "An overview of vibration and seismic application of NiTi shape memory alloy", *Smart Mater. Struct.*, **11**(2), 218-29.

SAC Joint Venture (1997), "Protocol for fabrication, inspection, testing and documentation of beam-column connection tests and other experimental specimens", Report no. SAC/BD- 97/02.

Song, G., Ma, N. and Li, H.N. (2006), "Applications of shape memory alloys in civil structures", *Eng. Struct.*, **28**(9), 1266-74.
Speicher, M.S., DesRoches, R. and Leon, R.T. (2011), "Experimental results of a Ni-Ti shape memory alloys (SMA)-based recentering beam'-column connection", *Struct. Eng.*, **33**(9), 2448.
Tyber, J., McCormick, J., Gall, K., DesRoches, R., Maier, J.H. and Abdel Maksoud, A.E. (2007), "Structural engineering with NiTi", *Basic Mater. Character. J. Eng. Mech.*, **133**, 1009-18.
Wang, W., Chan, T. M., Shao, H. and Chen, Y. (2015), "Cyclic behavior of connections equipped with NiTi shape memory alloy and steel tendons between H-shaped beam to CHS column", *Eng. Struct.*, **88**, 37-50.
Wang, W., Chan, T.M. and Shao, H. (2015), "Seismic performance of beam'-column joints with SMA tendons strengthened by steel angles", *J. Constr. Steel Res.*, **109**, 61-71.
Wilson, J.C. and Wesolowsky, M.J. (2005), "Shape memory alloys for seismic response modification: a state-of-the-art review", *Earthq. Spectra*, **21**(2), 569-601.

CC